

Neural Network-based Symbol Detection in High-speed OFDM Underwater Acoustic Communication

Zhipeng Chen*, Zhiqiang He^{*,b}, Kai Niu*, and Yue Rong[†]

^{*}Key Laboratory of Universal Wireless Communications, Ministry of Education, Beijing University of Posts and Telecommunications (BUPT), Beijing, China

^bKey Laboratory of Underwater Acoustic Communication and Marine Information Technology, Ministry of Education, Xiamen University, Xiamen, China

[†]Department of Electrical and Computer Engineering, Curtin University, Bentley, WA 6102, Australia

Abstract—Comparing with the terrestrial wireless channel, underwater acoustic (UA) channel is severely affected by strong impulsive noise, time variation and frequency variation. Except for channel estimation and channel equalization, symbol detection (SD) is also a significant part in the procedure of signal processing. In this paper, we propose a multilayer perceptron (MLP) neural network-based algorithm to manage the symbol detection task in UA communication. The neural network can learn more characters of UA channel and perform the task of signal processing effectively. From the view of MLP, the problem of constellation demodulation can be considered as an estimation of output symbols' probability. The cross entropy and rectified linear unit (ReLU) are used as loss function and activation function respectively. The traditional least-squares (LS) estimation and blanking combined with MLP-based symbol detection can have better performance on symbol-error-rate (SER). The proposed model is evaluated through numerical simulations with different parameters and real data collected during a UA communication experiment in December 2015 in the estuary of the Swan River, Western Australia. The results show that the proposed algorithm has a better performance than the existing method.

Index Terms—OFDM, neural network, symbol detection, underwater acoustic communication

I. INTRODUCTION

It is well known that underwater acoustic (UA) channel is one of the most challenging channels compared with terrestrial wireless communication channels. Due to the characteristics of the acoustic signal and severe underwater environment, the UA channel has large delay, significant Doppler shift, strong multi-path fading, and limited bandwidth [1],[2]. The UA channel has the character of dispersion in frequency and time domains. The relative movement of transmitter and receiver, as well as the motion of water, lead to frequency-domain dispersion. The time-domain dispersion due to delay spread results in severe inter-symbol interference. Therefore, an efficient channel estimation is important for high-speed UA communication system [4].

UA communication has made great advances in past decades [5],[6]. Orthogonal frequency-division multiplexing (OFDM) technique has attracted much research attention and been extensively applied in UA communication systems [7].

OFDM can eliminate the inter-symbol interference which is caused by multipath propagation by adding cyclic prefix and transferring the serial data stream to the parallel one to expand symbol period [3]. In addition, OFDM permits subcarrier overlapping on frequency spectrum to increase the spectral efficiency. Therefore, the application of OFDM in UA communication enables an improved spectral efficiency.

In recent years, machine learning (ML) and deep learning (DL) have been successfully applied in various fields such as computer vision (CV), natural language processing (NLP), speech recognition and so on. In some detection tasks, it has been demonstrated that the DL algorithms complete task beyond human's level of accuracy [8],[9]. From a DL point of view, a communications system can be seen as a particular type of autoencoder [10]. The application of DL in the physical layer of traditional communication has been discussed in [11],[12]. Among them, channel estimation and channel equalization are two main research directions. From the DL view, the procedure of passing channel can be regarded as conditional probability and the symbol decision at the terminal can be transferred to the problem of classification. In some specific scenes, the DL algorithms have better performance than traditional ones such as least-squares (LS) and least mean squares (LMS) algorithms [13].

It is known to all that channel estimation and equalization are important parts of receiver signal processing. Moreover, the symbol detection (SD) is also an important part of channel compensation.

In this paper, we propose a new algorithm which combines channel estimation with MLP-based SD. The MLP neural network has easier structure than convolutional neural network (CNN) and recurrent neural network (RNN). Since the MLP is fit for data with identical distribution, we first adopt least-square (LS) or orthogonal matching pursuit (OMP) to perform channel estimation. Then we use MLP as the SD module. The combination of traditional method with DL can achieve a better performance on SER.

The effect of the proposed algorithm is proved by numerical simulations and real data collected during a UA communication experiment conducted in December 2015 in

the estuary of the Swan River, Western Australia. The results show that compared with existing methods, the proposed algorithm has performance improvement in terms of bit-error-rate (BER), frame-error-rate (FER) and spectrum efficiency.

This paper is organized as follows: In Section II, the OFDM system model and the structure of the frame are presented briefly. In Section III, the structure of MLP and its methods of training are introduced in detail. In Section IV, the simulation and underwater experiment results are shown and discussed. Section V concludes the whole paper.

II. SYSTEM MODEL

The OFDM system we used contains N_c subcarriers of which N_d subcarriers are arranged for data information, N_p subcarriers are uniformly distributed to conduct channel estimation, N_{null} null subcarriers are used for avoiding the interference from out-of-band signals, N_{cfo} subcarriers are used for the estimation of frequency offset.

Each transmitted data frame consists of L_s OFDM symbols and 1 synchronization sequences (represented as training in Fig. 1 for the purpose of detecting the head of each data frame. The m sequence is considered as the synchronization sequence on account of its excellent character of autocorrelation. The structure of the frame is shown in Fig. 1.

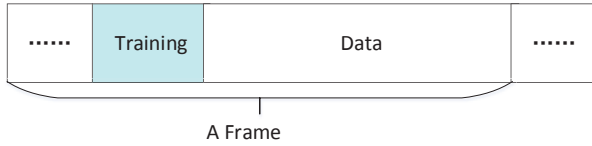


Fig. 1. The structure of a frame

The diagram of the UA OFDM system is shown in Fig. 2, the information bits $b(t)$ are mapped into symbols by Turbo coding and modulation constellation. The insertion of the pilot is used for synchronization and channel estimation. The IFFT operation transforms the signal from the frequency domain to the time domain. The function of cyclic prefix (CP) it to eliminate Inter-symbol Interference (ISI) caused by multipath fading. The effect of synchronization sequence (abbreviated as syn sequence in the diagram) is to find out the starting positing of a frame. Upsampling means we can get more data from one data point to improve the resolution so that we can accurately estimate the character of UA channel. The baseband signal can be expressed as

$$\mathbf{x} = \mathbf{F}^H \mathbf{d} \quad (1)$$

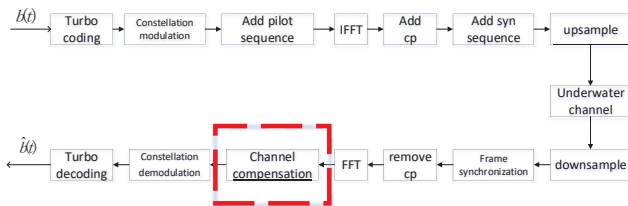


Fig. 2. Block diagram of OFDM UMA system

where \mathbf{F} is an $N_c \times N_c$ matrix for discrete Fourier transform (DTF), $(\cdot)^H$ stands for Hermitian transpose, The \mathbf{d} denotes the data vector.

The procedure of the receiver is reverse to that of the transmitter. Frame synchronization gets the initial position of each frame. It needs to be emphasized that the most important part of the OFDM is channel compensation, which is surrounded by the red broken line in Fig. 2. ‘‘channel compensation’’ contains channel estimation, channel equalization and SD. We use LS algorithm and zero force (ZF) algorithm to carry out the channel estimation and equalization. Then, the MLP-based model is used for SD. The neural network based algorithm is presented in detail in the next section.

In the transmitter, the passband signals are directly generated for each OFDM block. The bandwidth $B = f_{sc}N_c$ and the duration of the OFDM symbols is denoted as $T = 1/f_{sc}$. The frequency of the k -th subcarrier can be represented as

$$f_k = f_c + kf_{sc}, k = -\frac{N_c}{2} + 1, \dots, \frac{N_c}{2} \quad (2)$$

where f_c means the center carrier frequency. The time of duration of OFDM block can be represented as $T_{total} = T + T_{cp}$. T_{cp} denotes the duration of CP. The baseband signal can be expressed as

$$m(t) = \frac{1}{\sqrt{N_c}} \sum_{k=-\frac{N_c}{2}+1}^{\frac{N_c}{2}} \hat{d}[k] e^{j2\pi k f_{sc} t} \quad (3)$$

Adopting the complex envelope function, we have

$$\tilde{x}(t) = \begin{cases} 2\text{Re}\{m(t)e^{j2\pi f_c t}\}, & 0 \leq t \leq T \\ \tilde{x}(t+T), & -T_{cp} \leq t < 0 \end{cases} \quad (4)$$

where $\text{Re}\{\cdot\}$ denotes the real part of a complex number. According to [14], we assume that the path gains, Doppler scaling factors and multipath delay remain constant in an OFDM block. In addition, different paths have the same Doppler scaling factor a . Therefore, the UA channel which has L paths can be expressed as

$$h(t) = \sum_{l=0}^{L-1} A_l \delta(t + at - \tau_l) \quad (5)$$

where A_l and τ_l denote amplitude and delay of the the l th path respectively. Without considering the frequency offset, the received signal can be expressed as

$$\mathbf{r}_f = \mathbf{\Delta} \mathbf{h}_f + \mathbf{v}_f + \mathbf{n}_f \quad (6)$$

where $\mathbf{\Delta}$ means the diagonal matrix whose elements on diagonal are signal components. \mathbf{v} and \mathbf{n} denote impulsive noise and environment respectively and

$$\mathbf{h}_f = \mathbf{F} \mathbf{h}_t, \mathbf{v}_f = \mathbf{F} \mathbf{v}_t, \mathbf{n}_f = \mathbf{F} \mathbf{n}_t \quad (7)$$

III. THE PROPOSED ALGORITHM

In this section, we propose an MLP-based algorithm to perform the procedure of symbol detection. As shown in Fig. 2, ‘‘channel compensation’’ is an important process in the whole OFDM procedure. In Fig. 3, we describe the

content of “channel compensation” in detail. In general, it includes three submodules: channel estimation, channel equalization and symbol detection (SD).

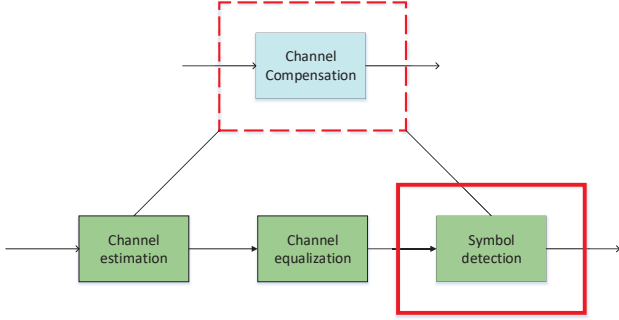


Fig. 3. The detail of channel compensation

Channel estimation and equalization can adopt the classical LS algorithm and ZF algorithm for simplicity. Compressed Sensing (CS), Orthogonal Matching Pursuit (OMP) and minimum mean-square error (MMSE) can also be adopted for better performance. We will show that the proposed DL based SD algorithm can improve the system performance for UA OFDM with both classical and advanced channel estimation and equalization algorithms. Channel estimation makes use of pilot carrier and interpolation to obtain channel impulse response in other position. Channel equalization eliminates the time selective fading and frequency selective fading. We don't discuss the detail of channel estimation and equalization algorithm due to limited space.

We use the MLP neural network to perform the part of symbol detection, which is labeled in Fig. 3 by the red solid color rectangular box. The structure of the neural network is illustrated in Fig. 4. Data after estimation and equalization is sent to the MLP neural network, which is trained by either simulated data or data collected from real UA communication experiments.

In our specific scene, MLP is trained to solve a 4-class decision problem because we chose a QPSK modulation constellation and the 4 outputs correspond to 4 kinds of symbols. We train the model on Tensorflow and Keras, which can greatly simplify the procedure of training and adjusting parameters. The input data includes real part and imaginary part and they are reshaped into a vector whose dimension is relevant to the number of nodes in the input layer.

The training steps are illustrated as:

- 1) Set the initial value of weight by randomization and set the value of hyper-parameters.
- 2) Choose the activation function
- 3) Set the shape of the loss function
- 4) Accomplish the construction of MLP network and launch the training

The input data include real part and imaginary part, which are reshaped and concatenated into a vector as input data. The elements on hidden layer 1 can be computed as

$$n_j = \sum_{i=0}^N U_i w_{ij}, \forall i \in 1, 2, \dots, N \quad (8)$$

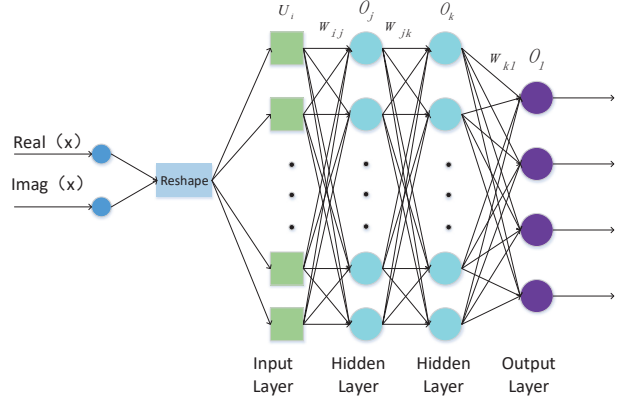


Fig. 4. The structure of MLP neural network

$$O_j = \varphi(n_j) \quad (9)$$

where w_{ij} is the weight between the i th input node and the j th hidden node. U_i denotes the input information on the i th input neuron. $\varphi(\cdot)$ represents the ReLU activation function. N is the number of neurons in the input layer. We choose the ReLU as the activation function rather Sigmoid because the latter has the slower rate of convergence and are prone to causing the problem of “gradient vanishing”.

We adopt the ReLU as activation function and its expression is:

$$\varphi(x) = \begin{cases} 0 & , x \leq 0 \\ x & , x > 0 \end{cases} \quad (10)$$

The data on the second hidden layer can be expressed as:

$$n_k = \sum_{j=0}^{L_1} O_j w_{jk}, \forall j \in 1, 2, \dots, L_1 \quad (11)$$

$$O_k = \varphi(n_k) \quad (12)$$

In our scene, the problem is defined as a K -class decision problem and $K = 4$. Therefore we adopt SoftMax activation function to acquire the outputs for the output layer. L_1 means the number of neurons in the first hidden layer. The output results are computed as:

$$O_l = f(n_l) = f\left(\sum_{k=0}^{L_2} O_k w_{kl}\right), \forall k \in 1, 2, \dots, L_2 \quad (13)$$

L_2 means the number of neurons in the second hidden layer. $f(\cdot)$ denotes SoftMax activation function, whose expression can be expressed as:

$$f(n_l) = \frac{e^{n_l}}{\sum_{m=1}^K e^{n_m}}, \forall l \in 1, 2, \dots, K \quad (14)$$

As for the loss function, we use the cross-entropy function, which is a classical loss function and combined with SoftMax function. Its expression is:

$$loss = -\frac{1}{m} \left[\sum_{i=1}^m \sum_{j=1}^K I(x^{(i)} = j) \log f(n_j) \right] \quad (15)$$

where m is the total number of training examples and $I(\cdot)$ means Indicator function, which signifies $I(A = B)$ return 1 if and only if A is equal to B.

According to equations (7)-(11), we can receive the MLP output is:

$$O_l = f(n_l) = f\left(\sum_{k=0}^{L_2} w_{kl} \varphi\left(\sum_{j=0}^{L_1} w_{jk} \varphi\left(\sum_{i=0}^N w_{ij} U_i\right)\right)\right) \quad (16)$$

The output data is sent to the demodulation module and the following steps will be conducted. We debug parameters of MLP by setting fixed step length and carry out grid research. Then, we choose a group of parameters which make the systems have best performance. Key parameters are shown in Table I.

TABLE I
PART OF PARAMETERS OF MLP NETWORK

Input size	24
Output size	4
Number of hidden layers	2
Number of neuron in hidden layer 1	10
Number of neuron in hidden layer 2	10
Batch size	1024
Dropout	0.25

IV. EXPERIMENT RESULTS

In this section, the performance of the proposed model is evaluated through numerical simulations and data collected from the underwater environment. Part of the simulation parameters are shown in Table II. According to Table II,

TABLE II
PARAMETERS SETTING IN SIMULATION

Total number of subcarriers	512
Number of Data subcarriers	325
Number of Pilot subcarriers	128
Number of Null subcarriers	59
Channel coding	Turbo
Code rate	1/3
Constellations modulation	QPSK
Number of bits in one frame(considering code puncturing)	1088
Number of multipath	15
Delay between two adjacent path	1ms

the number of bits in one frame is $L_b = 1088$. Therefore, the data rate of the system can be expressed as

$$R_b = \frac{L_b}{(T + T_{cp})(N_b + 1)} = 1.19kb/s \quad (17)$$

Considering the under practical environment, we adopt the Gaussian mixture model in [14]. The underwater noise concludes background noise and impulsive noise. Therefore, the probability density function(pdf) can be written as:

$$pN(0, \sigma_1^2) + qN(0, \sigma_2^2) \quad (18)$$

where $N(0, \sigma^2)$ denotes a complex Gaussian probability function whose average is 0 and variance is σ^2 . σ_1^2 is the variance of background noise and σ_2^2 is the variance of the

impulsive noise. The parameter of p and q are weights of two kinds of noise. As a result, the signal-to-noise ratio (SNR) can be expressed as:

$$SNR = \frac{P_s}{p\sigma_1^2 + q\sigma_2^2} \quad (19)$$

where P_s is the average power of the transmitted signal. In our simulation, we set $p = 0.98$, $q = 0.02$, the power ratio of two kinds of noise is σ_2^2/σ_1^2 , P_s is equal to 1 because of the normalization of the modulation symbol's power.

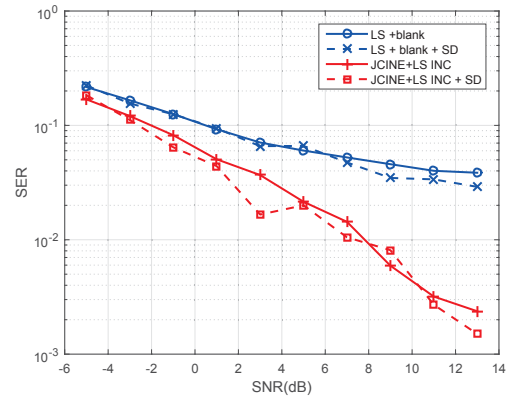


Fig. 5. The locations of transmitter and receiver

The joint channel and impulsive noise estimation (JCINE) algorithm has been introduced in [15]. It uses OMP performing Channel estimation and makes fully use of sparsity of channel impulse response. The SER performance of various algorithms versus the SNR is shown in Fig. 5. It can be seen that proposed models have better performance than existing ones because of lower SER. However, it can be seen that proposed algorithm has worse performance on some points. The variation of the channel is the main reason of the phenomenon.

The proposed model is applied to deal with underwater data, which is collected in the UA communication experiment conducted in December 2015 in the estuary of the Swan River, Western Australia. The distance between the transmitter and receiver are 936 meters and their location is marked in Fig. 6 In addition, the transmitter transducer and the receiver hydrophone are mounted above the river bed on steel frames, which are cabled to shore to avoid the effect of Doppler shift in the experiment. The background noise principally includes an impulsive component from snapping shrimp and waves against the shore. The key parameters are summarized in Table III. Each transmission includes 500 data frames, of which 250 data frames conveyed 1088 information bits(1/3 rate code) and 250 data frame contained 1632 information bits(1/2 code rate). The data between the transmitter and receiver is recorded and named as T83. The performance of the proposed model and comparison are shown in the Table IV

- LS channel estimation without blanking
- LS channel estimation with blanking



Fig. 6. The locations of transmitter and receiver

TABLE III
PART OF PARAMETERS OF THE EXPERIMENTAL SYSTEM

bandwidth	B	4kHz
Carrier frequency	f_c	12kHz
Sampling rate	f_s	96kHz
Subcarrier spacing	f_{sc}	7.8Hz
Length of OFDM symbol	T	128ms
Length of CP	T_{cp}	25ms
Number of blocks in one frame	N_b	5

- LS channel estimation with blanking and SD
- JCINE algorithm with LS based INC [15]
- JCINE algorithm with LS based INC and SD

TABLE IV
PERFORMANCE COMPARISON OF VARIOUS ALGORITHMS FOR THE T83
FILE(QPSK MODULATION)

Method	SER	RAW BER	Coded BER	FER
LS w/o blanking	11.27%	6.2%	0.16%	0.4%
LS + blanking	9.68%	5.2%	0	0
LS + blanking +SD	6.55%	-	-	-
JCINE + LS INC	6.61%	3.5%	0	0
JCINE + LS INC +SD	4.1%	-	-	-

It can be seen from the results that the model we proposed can obtain lower SER when it combines with other algorithms. It introduces 3% decrease in SER after blanking and 2.5% decrease in SER after JCINE. “-” means no results available. We can conclude that the proposed model has a better performance than existing models.

V. CONCLUSION

In this paper, we propose an MLP-based algorithm to perform symbol detection. The symbol detector locates in the position after channel estimation and channel equalization but before modulation constellation. The MLP can adequately extract the feature of the underwater channel and improve performance on SER and BER. Our results are compared to traditional methods without symbol detection and have better performance on simulation as well as underwater experiment data.

REFERENCES

- [1] A.C. Singer, J. K. Nelson, and S. S. Kozat, “Signal processing for underwater acoustic communications,” *IEEE Commun.Magazine*, vol. 47, no. 1, pp. 90-96, Jan. 2009.
- [2] D. B. Kilfoyle and A. B. Baggeroer, “The state of the art in underwater acoustic telemetry,” *IEEE J. Ocean. Eng.*, vol. 25, no. 1, pp.4-27, Jan. 2000.
- [3] M. Stojanovic, “Low complexity OFDM detector for underwater acoustic channels,” in *Proc. MTS/IEEE OCEANS*, Boston, USA, Sep. 2006.
- [4] W. Li and J. C. Preisig, “ Estimation of rapidly time-varying sparse channels,” *IEEE J. Ocean. Eng.*, vol. 32, no. 4, pp. 927-939, Oct. 2007.
- [5] M. Stojanovic, L. Freitag, and M. Johnson, “Channel-estimationbased adaptive equalization of underwater acoustic signals,” in *Proc. MTS/IEEE OCEANS*, Seattle, WA, USA, 1999.
- [6] M. Stojanovic and L. Freitag, “Multichannel detection for wideband underwater acoustic CDMA communications,” *IEEE J. Ocean. Eng.*, vol. 31, no. 3, pp. 685-695, Jul. 2006.
- [7] B. Li, S. Zhou, M. Stojanovic, and L. Freitag, “Pilot-tone based ZP-OFDM demodulation for an underwater acoustic channel,” in *Proc.MTS/IEEE OCEANS*, Boston, MA, USA, 2006.
- [8] Y. LeCun et al., “Generalization and network design strategies,” *Connectionism in perspective*, pp.143-155, 1989.
- [9] K. He, X. Zhang, S. Ren, and J. Sun, “Delving deep into rectifiers:Surpassing human-level performance on imagenet classification,” in *Proc. IEEE Int. Conf. Computer Vision*, 2015, pp.1026-1034.
- [10] I. Goodfellow, Y. Bengio, and A. Courville, *Deep Learning*. MIT Press, 2016
- [11] H. Ye, G. Y. Li and B. H. Juang, “Power of Deep Learning for Channel Estimation and Signal Detection in OFDM Systems,” *IEEE Wireless Communications Letters* vol.7, no.1, pp.114-117, Feb.2018.
- [12] Y. Li, M. Chen, Y. Yang, M. T. Zhou and C. Wang, “Convolutional recurrent neural network-based channel equalization: An experimental study,” in *emphAsia-Pacific Conference on Communications (APC-C)*, Perth, WA, 2017.
- [13] MN. Seyman, et al “Channel estimation based on neural network in space time block coded MIMO-OFDM system,” *Digital Signal Processing*, vol.23, no.1, pp.275-280, 2013
- [14] X. Kuai, H. Sun, S. Zhou, and E. Chen, “Impulsive noise mitigation in underwater acoustic OFDM systems,” *IEEE Trans. Veh. Technol.*, vol.65, no.10, pp.8190-8202, Oct.2016
- [15] P. Chen, Y. Rong, S. Nordholm and Z. He, “Joint Channel and Impulsive Noise Estimation in Underwater Acoustic OFDM Systems,” *IEEE Transactions on Vehicular Technology*, vol. 66, no. 11, pp. 10567-10571, Nov. 2017.